

ICM11

## DEVELOPMENT OF DENSE AND CELLULAR SOLIDS IN $C_R C_O M_O$ ALLOY FOR ORTHOPAEDIC APPLICATIONS

Sergio Rivera<sup>1</sup>, María Panera<sup>1</sup>, Daniel Miranda<sup>1</sup>, F.J. Belzunce Varela<sup>2</sup>

<sup>1</sup>Fundación ITMA. Parque Empresarial del Principado de Asturias (PEPA), Calafates, S/N, parcela L-3.4, 33400 Avilés, Asturias.  
[s.rivera@itma.es](mailto:s.rivera@itma.es), [m.panera@itma.es](mailto:m.panera@itma.es)

<sup>2</sup>Departamento de Ciencia de los Materiales e Ingeniería Metalúrgica. Universidad de Oviedo. Campus universitario, 33203 Gijón, Asturias.  
[belzunce@uniovi.es](mailto:belzunce@uniovi.es)

---

### Abstract

SLS (Selective laser sintering) is a rapid prototyping technique used for the development of new biomaterials with application in implantology. In the present work, dense and cellular solids have been obtained by this technique. Firstly, the sintering direction for obtaining dense solids has been studied and porosity, microstructure and mechanical properties resulting of the different sintering orientations have been evaluated. The vertical orientation in the sintering process generates higher porosity that results in poor fatigue properties, so a HIP treatment is proposed in order to overcome the problem. A conventional HIP treatment results in a homogenization of the properties independently of the sintering orientation. Secondly, a porous (Cellular) structure was obtained with a pore size of about 0.5 mm and an elevated interconnectivity. The structural and mechanical properties have been obtained by means of scanning electron microscopy and compression testing, resulting in very similar results to that obtained in commercial metallic cellular materials.

© 2011 Published by Elsevier Ltd. Open access under [CC BY-NC-ND license](https://creativecommons.org/licenses/by-nc-nd/4.0/).  
Selection and peer-review under responsibility of ICM11

Key Words: Biomaterials, Selective Laser Sintering; Implantology.

---

### 1. INTRODUCTION

Rapid prototyping techniques for the development of biomaterials are being nowadays widely used and are considered an alternative to the traditional processes of casting and forging [1]. CAD/CAM based layered manufacturing techniques are specially applicable when near net shape components must be performed. This is for example the case when a complex implant geometry must be manufactured or when some specific functionalities must be added to the component in order to enhance the mechanical biocompatibility, for example a porosity gradient [2]. The most important metallic biomaterials obtained by means of these techniques are titanium, tantalum, cobalt-chromium alloys and stainless steels. Several components made of these materials are traditionally used in high load bearing applications where mechanical properties are critical. The typical materials are titanium and its alloys and also cobalt alloys, mainly the standard quality ASTM F75 [3]. Implants made of these materials are used

for total hip replacements (THR); titanium alloy in the stem femoral component, cobalt alloys in the femoral heads and both alloys in the acetabular component [4].

At present, one of the solutions adopted in THR is the double mobility concept [5], based in the use of a three components system with two friction surfaces. The principle of double mobility for the acetabular component has several advantages like a higher joint stability that leads to a lower dislocation risk [6], but present the problem of having two friction surfaces (metallic versus polyethylene as the most typical), that produce debris to the physiological medium. These particles are mainly produced at the interface of the femoral head against the polyethylene bearing, and are responsible of the osteolysis and aseptic loosening [7]. Some of the traditional acetabular shells are made of a hard material, like cobalt alloys, provided of a surface coating of some porous material to enhance the biological fixation of these implants to the bone. These coatings have some limitations such as a low volumetric porosity, a relatively high Young modulus and low wear properties [8,9].

In order to cope to the limitations of this technology, a new concept of acetabular shell has been developed in the course of the last years, based on an innovative design with a functionally graded acetabular shell with open porosity in the side in contact with the bone to improve cell-materials interactions and a hard alloy on the other side with good properties against wear. This kind of porous surfaces increase the bone contact, enhances primary stability and also cellular proliferation and angiogenesis, through their typical interconnected cellular structure [11]. The porous tantalum open-cell structure (Zimmer, Trabecular Metal Technology, Inc., Parsippany, NJ) developed by Zimmer consists on a tantalum material that is deposited onto an interconnected vitreous carbon scaffold using vapour deposition techniques. An orthopedic application of a monoblock acetabulum component has been performed using this technique.

On the other hand, rapid prototyping techniques have been applied for the manufacturing of these components. Lima corporate has the Delta TT solution [12], a porous titanium acetabular component made by electron beam melting (EBM) with a 3D structure made by hexagonal cells. It has an extremely low Young modulus in the porous part (1.2 GPa) with a porous diameter of 0.64 mm and an interconnected structure. Dittrick et al. have developed functionally graded materials using laser engineering net shaping (LENS) processes with a hard and wear resistant coating of a CoCrMo alloy on a porous titanium structure, having demonstrated the possibility to be used in these applications. The problem of this solution is due to diffusion phenomena, that leads to the formation of brittle phases that can induce the premature fracture of the component.

In the present work, a selective laser sintering process developed by the company EOS has been used for obtaining porous (cellular) and dense CoCrMo alloys. The effect of product orientation in the sintering process has been studied and, in the case of the vertical orientation process, the effect of a HIP (hot isostatic pressing) treatment was evaluated. The properties of all these products have been compared.



Fig 1. From left to right. Delta TT solution for acetabular part; Zimmer monoblock tantalum component; Interconnected porosity of Trabecular Metal™ of Zimmer.

## 2. MATERIALS AND METHODS

### 2.1. Processing

#### 2.1.1. Dense material

Rapid prototyping manufacturing has been performed in an M270 EOSINT machine, using the selective laser sintering technique and EOS CobaltChrome raw material[13]. Cylindrical specimens with a diameter of 10 mm and a total length of 100 mm were sintered. Two different routes of fabrication varying the sintering orientation have been analyzed; “x-y” when the specimen longitudinal axis was in the horizontal direction; “z” when the longitudinal axis of the specimen was in the vertical direction. After the sintering process, some of the specimens were hot isostatically pressed (HIP), during 240 minutes at 1200°C under a pressure of 103 MPa. Two cooling routes were programmed:

- slow controlled cooling to 4.2 – 4.5 °C/min (HT1).
- A variable cooling, with a free cooling from 1200°C to 720 °C in 15'27'' (33°C/s) and a subsequent cooling rate of 10 °C/min (HT2) up to room temperature.

#### 2.1.2. Porous material

Five specimens were sintered to form a porous CoCrMo product onto a dense steel substrate. Porous material specimens were cylindrical with a height of 2 mm and a diameter of 14 mm. By means of the selective laser sintering process, a close control of variables such as pore size, morphology, volume percent and pore interconnectivity is obtained.

### 2.2. Chemical and physical properties

One sample of the sintered dense cylinders was cut in a transversal plane and a chemical analysis of the material was performed using spark emission spectrometry. It was considered that the sintering orientation does not affect the bulk chemical composition of the material. The chemical composition of the porous product was measured by means of inductively coupled plasma mass spectroscopy (ICP-MS). The real density of the dense material and the porosity of the porous structure were obtained using an helium pycnometer. The value of the density of the dense material consisted on the average of three different measurements obtained from specimens sintered in both orientations (“x-y” and “z”) and also of three sintered and HIP treated specimens (HT1). The density of the porous material was measured using only one single specimen.

### 2.3. Mechanical Properties

Tensile tests were performed to the dense material following the requirements of the UNE-EN 10002-1 standard using an universal 8801 Instron testing machine provided of a load cell of 100 kN. Seven conditions were evaluated by means of a set of three tests for each one:

- “as-sintered x-y”.
- “as-sintered z”.
- “as-machined x-y”: sintered in the “x-y” orientation and then machined to a mirror polished surface condition.
- “as-machined z”: sintered in the “z” orientation and then machined to a mirror polished surface condition.
- “HT1 x-y”: Sintered in the “x-y” orientation, HIP treated (HT1 cooling) and then machined to a mirror polished surface condition.
- “HT1 z”: Sintered in the “z” orientation, HIP treated (HT1cooling) and then machined to a mirror polished surface condition.

- “HT2 z”>: Sintered in the “z” orientation, HIP treated (HT2 cooling) and then machined to a mirror polished surface condition.

The “as-sintered” specimens have a cylindrical geometry, with a diameter in the reduced cross section of 10 mm. The geometry of the remaining specimens had a final diameter in the reduced cross section of 5 mm. In all cases, for the measurement of the elongation, a static axial clip-on extensometer with an initial length of 25 mm was used.

Fatigue tests were performed on the dense material following the requirements of the ASTM E466 [14] standard in an 8801 Instron universal testing machine, with a load cell of 10 kN, using a load control condition with a sinusoidal wave of 0-400 MPa and a test frequency of 20 Hz. A run-out limit of 8 million of cycles was set up, so that the tests that attained this number of cycles were stopped and considered to have an infinite fatigue life. A set of three specimens were tested for each one of the following conditions:

- “as-machined x-y”>: sintered in the “x-y” orientation and then machined to a mirror polished surface condition.
- “as-machined z”>: sintered in the “z” orientation and then machined to a mirror polished surface condition.
- “HIP x-y”>: sintered in the “x-y” orientation, HIP treated (HT1 cooling) and then machined to a mirror polished surface condition.
- “HIP z”>: sintered in the “z” orientation, HIP treated (HT1 cooling) and then machined to a mirror polished surface condition.

On the other hand, compression tests were performed to four specimens of the porous material in order to obtain the Young modulus and the maximum compression strength. An 5582 Instron universal testing machine with a load cell of 10 kN was used. The test set-up was composed by two compression plates and a static clip-on extensometer with an initial length of 10 mm, which was located at a distance of 4 mm from each one of the porous material surfaces in order to minimize the system compliance. A test rate of 1 mm/min was employed and the final test event was a load decrease of 5 %.

Additionally, Vickers hardness measurements were performed in one of the porous specimens. Two different samples were prepared, one in the transversal orientation and the other in the longitudinal orientation. The samples were mounted in resin and polished to a mirror condition. The measurements were performed by means of a L400 Leco micro-hardness tester, with a load of 1 kg and following the requirements of the UNE-EN ISO 6507-1 standard.

#### 2.4. Microstructure

The microstructure of the dense material was evaluated in the sintered condition in both orientations “x-y” and “z”. Samples in the horizontal and transversal orientation with respect to the longitudinal axis of the cylinder were cut and prepared. These samples were polished to a mirror condition and then analyzed in an optical microscope for a quantitative determination of the porosity (ten different fields). Afterwards, the specimens were chemically etched with oxalic acid in order to reveal the microstructure. The same procedure, except for the porosity, was done with a sample of the “HIP x-y” condition.

The microstructure of the porous material was studied by means of scanning electron microscopy. A two dimensional analysis of the structure was performed in order to evaluate the mean pore size and its interconnectivity. For determining the average pore size, ten different fields was evaluated. Furthermore, a transversal cut of one of the sintered porous specimens was mounted in resin and observed under the optical microscope.

### 3. RESULTS

#### 3.1. Dense material

The chemical composition of the dense material (see Table 1) is comprised into the valid range stated in the ASTM F75-01 standard, so the SLS process is valid from this point of view as an alternative process to the traditional routes of fabrication. Helium porosimetry was not a valid method to measure the internal porosity of the material and only gives a single value of the theoretical density. After HIP treatments, the theoretical density increases a 0.3% in the “x-y” orientation and 0.15 % in the “z” orientation with respect to the “as-sintered” material.

The performed porosity analysis showed that porosity had a random distribution, but the “as-sintered z” orientation, had a porosity three times higher than in the “as-sintered x-y” orientation. The maximum pore size in both sintering orientations is similar, with an approximate average size of 60-80  $\mu\text{m}$  and an irregular geometry. The acid etching has revealed a single phase microstructure with a characteristic morphology of the laser sintering process (see Fig. 2).

The four hours 1200°C holding of the HIP treatment (HT1) results in the destruction of the as-sintered microstructure and a clear grain growth until a 5 ASTM grain size (mean size of 63  $\mu\text{m}$ ). During cooling, chromium and molybdenum carbides precipitate in grain boundaries due to the slow cooling rate used in HT1. HIP HT2 treatment, with a fast cooling rate from 1200°C to 720°C, was performed in order to avoid this massive carbide precipitation, but cooling rate was not high enough to obtain the required results.

The tensile properties reflect a clear influence of the material porosity, as the samples sintered in the “z” orientation had worse properties than in the “x-y” orientation. A decrease in the yield strength, maximum tensile stress and elongation was observed (Table 2). The surface quality of the samples in the as-sintered condition strongly penalizes the tensile properties, so that after machining a mirror polished surface, a significant increase of these properties were obtained. The HIP-HT1 treatment has achieved a homogenization of the mechanical properties of the products regardless the sintering orientation, but a decrease in the yield stress and tensile strength and an increase in the Young modulus and elongation has occurred. These results are consistent with the microstructure evolution already mentioned and show the influence of carbide precipitation in grain boundaries. Finally, the specimens treated in the HIP-HT2 cycle, provided by a fast cooling rate from 1200°C to 720°C, already attained a much higher elongation, in the order of the expected value for this material submitted to HIP.

The fatigue properties were highly penalized in the “z” sintering orientation because of the influence of the porosity, as fractures always took place below 300.000 cycles. The data consulted in the bibliography give a higher survival rate, even superior to 7 millions of cycles under these load conditions. This number of cycles is fulfilled by the “as-sintered x-y” condition. The fatigue failure of the specimens sintered in the “z” orientation was originated in sub-surface defects, probably due to the internal porosity generated during the sintering process. After HIP treatment, due to the densification provided, the fatigue properties do not depend on the sintering orientation and the run-out cycles are fulfilled for all sintering conditions.

Table 1. Chemical composition (% in weight).

Element	C (%)	Si (%)	Mn (%)	Ni (%)
as-sintered “x – y”	0.13	0.71	0.70	0.09
ASTM F75-01	0.35 máx	1.0 máx	1.0 máx	0.50 máx
Element	Cr (%)	Mo (%)	Fe (%)	Co (%)
Sint “x – y”	27.9	6.54	0.11	64
ASTM F75-01	27-30	5-7	0.75 máx	Bal



Table 2. Tensile results.

	$\sigma_{ys}$ (MPa)	$\sigma_R$ (MPa)	e (%)	E (GPa)
as-sintered "x-y"	917	1240	10	184
as-machined "x-y"	1018	1342	11.25	211
as-sintered "z"	740	1105	9	198
as-machined "z"	751	1194	-	204
HT1 "x-y"	667	1077	15.75	248
HT1 "z"	658	1046	16.75	248
HT2 "z"	629	1105	21.00	243

Table 3. Fatigue results.

	Specimen 1 (cycles)	Specimen 2 (cycles)	Specimen 3 (cycles)
as-machined "x-y"	$8 \cdot 10^6$	$8 \cdot 10^6$	$8 \cdot 10^6$
as-machined "z"	134.020	157.275	251.856
HT1 "x-y"	$8 \cdot 10^6$	$8 \cdot 10^6$	$8 \cdot 10^6$
HT1 "z"	$8 \cdot 10^6$	$8 \cdot 10^6$	$8 \cdot 10^6$

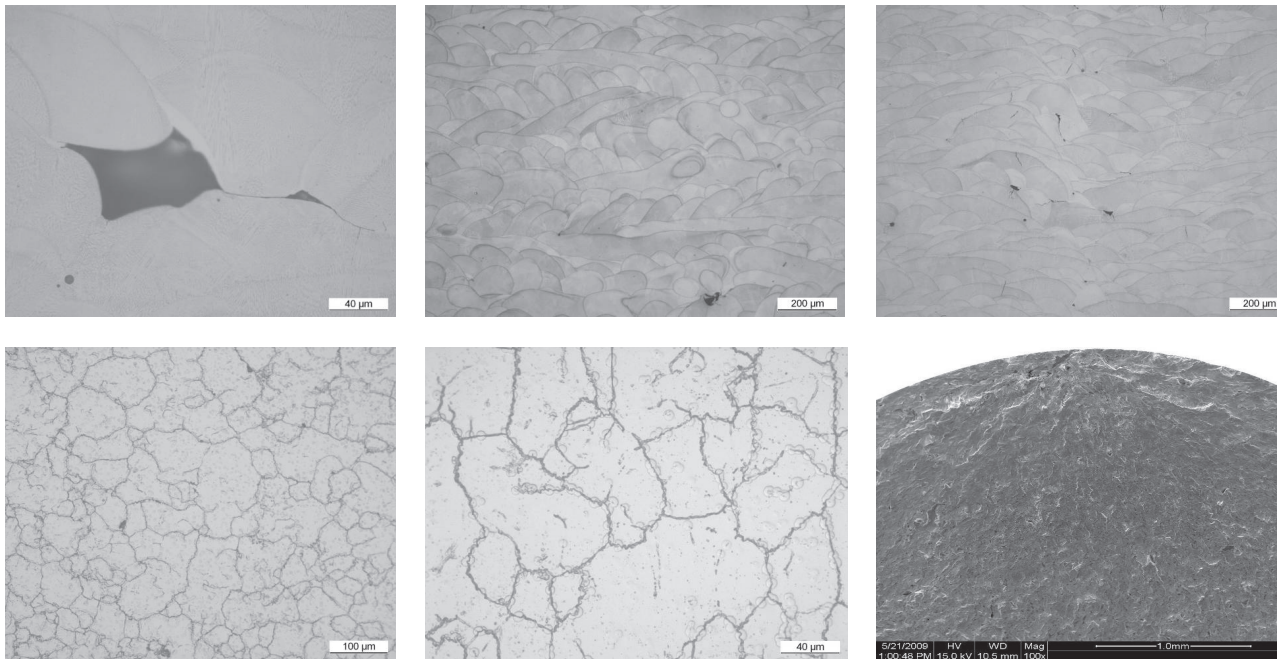


Fig 2. From left to right and top to bottom. Maximum pore size in the "as-sintered" condition (500x); microstructure of the "as-sintered x-y" condition (200x); microstructure of the "as-sintered z" condition (200x); microstructure of the "HT1 z" condition (100x); microstructure of the "HT1 z" condition (500x); fracture surface of the specimen 2 in the as-machined "z" condition (100x).

### 3.2 Porous Material

The chemical analysis performed on the porous material samples was satisfactory when it was compared with the range values of the standard composition (Table 4). The porous material had an interconnected structure with an average pore size of 475  $\mu\text{m}$  and a total open porosity of almost 80%. The Young modulus in compression has given a value of 1.5 GPa, the maximum compression stress was 85 MPa and a Vickers hardness of 485 HV was measured, with a high homogeneity. These values have been compared with commercial metallic bone substitutes made in other alloys (see Table 5) [15, 16]. The results presented in Table 5 show that the designed components performed in this porous material for orthopaedic application have a mean pore size, percent porosity, Young modulus and

maximum compression strength not much different from the values reported on commercial materials [17], and close to the bone properties [18, 19].

Table 4. Chemical composition of porous material (% in weight).

Element	C (%)	Si (%)	Mn (%)	Ni (%)
Porous material	-	0.70	0.60	0.07
ASTM F75-01	0.35 max	1.0 max	1.0 max	0.50 max
Element	Cr (%)	Mo (%)	Fe (%)	Co (%)
Porous material	29.0	5.96	0.16	63
ASTM F75-01	27-30	5-7	0.75 max	Bal

Table 5. Properties of the porous materials.

	CoCrMo Porous	Tantalum ( <sup>TM</sup> Zimmer)	Tritanium (Stryker)
Pore size ( $\mu\text{m}$ )	475	400 - 600	546
Porosity (%)	77	75 - 85	72
E (GPa)	1.5	2.5 - 3.9	-
$\sigma_{\text{Max}}$ (MPa)	85	50 - 110	-
HV1	438	279-345	-

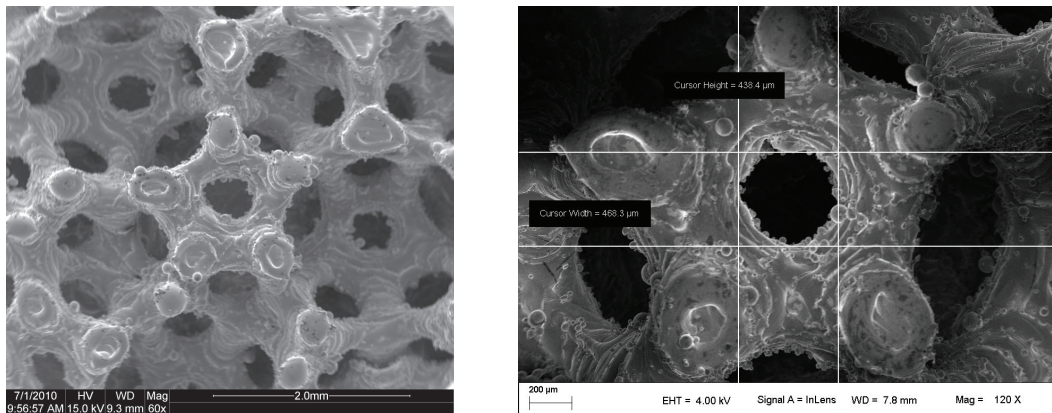


Fig 3. From left to right. Interconnectivity between pores; measurement of the pore sizes.

#### 4. CONCLUSIONS

The additive manufacturing process of dense CrCoMo alloys by selective laser sintering has resulted a validated technique for the fabrication of products to implantology. By selecting the appropriate parameters for the sintering process, good results in the “x-y” orientation have been achieved. The same parameters in the “z” orientation of sintering promotes an internal higher porosity that results in tensile and fatigue properties decrease with respect to the “x-y” orientation. The highest pore size is similar in both orientations (approximately 80  $\mu\text{m}$ ) and have a characteristic geometry that lead to high stress concentration factors. Anyway, the premature fatigue failures in the “z” orientation samples were mainly explained by their pores content and distribution, having a higher probability that a pore or pores close to the surface act as a crack nucleation site.

Applying a HIP treatment, the total densification of the material is obtained. After HIP treatment, the influence of the sintering direction in porosity and mechanical properties disappears completely. In this case, the use of standard parameters in the HIP cycle generates a decrease in the yield stress and tensile strength but an increase in the Young modulus and elongation with respect to the as-sintered samples. The high temperature applied during HIP process (1200°C) along with the long holding time at this temperature has resulted in a coarsening of the grain size, and the slow cooling rate in the case of the first heat treatment HT1 (4.2°C/min) led to an abundant grain boundary

carbide precipitation and this being the main reason for the observed decrease in the tensile properties. The use of a faster cooling rate in the HT2, give way to a higher tensile strength and elongation.

The porous CoCrMo alloy also produced by selective laser sintering had an interconnected porosity with a mean pore size, a total porosity and tensile properties close to the bone properties and similar to other metallic bone substitutes.

### **Acknowledgement**

The authors want to thank the company SOCINSER S.A., which have the property rights of the acetabular solution mentioned and also want to thank to the Oviedo University and Fundación Prodimtec as partners in this research project and of course to the regional government of Principado de Asturias (FICYT) for funding the aforementioned project.



## References

- [1] K. Alvarez, H. Nakajima. “Metallic scaffolds for bone regeneration”. *Materials* 2009, 2, 790-832.
- [2] John Alan Hunt, Jill T. Callaghan, Chris J. Sutcliffe, Rhys H. Morgan, Ben Halford, Richard A. Black. “The design and production of Co–Cr alloy implants with controlled surface topography by CAD–CAM method and their effects on osseointegration”. *Biomaterials* 26 (2005) 5890–5897.
- [3] ASTM F75-07: “Standard Specification for Cobalt-28 Chromium-6 Molybdenum Alloy Castings and Casting Alloy for Surgical Implants”.
- [4] S. Dittrick, V. Krishna Balla, N. M. Davies, S. Bose, A. Bandyopadhyay. “In vitro wear rate and Co ion release of compositionally and structurally graded CoCrMo–Ti6Al4V structures”. *Materials Science and Engineering C*. 2010. Article in press.
- [5] Bousquet G, SERF. Prothèse de l'articulation de la hanche. Evaluation de l'usure sur l'insert du cotyle à double mobilité.
- [6] Pr. Leclercq, P. Marechal, F. Menguy, J.H. Aubriot. High intrinsic stability achieved by the mobile liner, for recurrent dislocations indications. Repeating Dislocations Treatment with the Bousquet Cup SOFCOT, 1999.
- [7] Taddei, P.; Affatato, S.; Fagnano, C.; Toni, A. Oxidation in ultrahigh molecular weight polyethylene and cross-linked polyethylene acetabular cups tested against roughened femoral heads in a hip joint simulator. *Biomacromolecules* 2006, 7, 1912-1920.
- [8] Kurzweg, H. et al., Development of plasma-sprayed bioceramic coatings with bond coats based on titania and zirconia, *Biomaterials*, 19, 1507, 1998.
- [9] Nie, X. and Leyland, A., Deposition of layered bioceramic hydroxyapatite/TiO<sub>2</sub> coatings on titanium alloys using a hybrid technique of micro-arc oxidation and electrophoresis, *Surf. Coating Tech.*, 125, 407, 2000.
- [10] Johansson CB, Hansson HA, Albrektsson T. Qualitative interfacial study between bone and tantalum, niobium or commercially pure titanium. *Biomaterials* 1990;11:277–80.
- [11] R. Singh, P.D. Lee, T.C. Lindley, C. Kohlhauser, C. Hellmich, M. Bram, T. Imwinkelried, R.J. Dashwood. Characterization of the deformation behavior of intermediate porosity interconnected Ti foams using micro-computed tomography and direct finite element modeling. *Acta Biomaterialia* 6 (2010) 2342–2351.
- [12] Trabecular Tritanium™. Naturae Imitatio. Lima Corporate.
- [13] Eos CobaltCrome MP1 for EOSINT M270.
- [14] ASTM E466-02 “Standard practice for conducting force controlled constant amplitude axial fatigue tests of metallic materials”
- [15] Trabecular Metal™ Technology. Zimmer.
- [16] Tritanium Primary Acetabular Shell. Stryker.
- [17] Lyle D. Zardiackas, Douglas E. Parsell, Lance D. Dillon, Darrell W. Mitchell, Laura A. Nunnery, Robert Poggie. “Structure, Metallurgy, and Mechanical Properties of a Porous Tantalum Foam”. *Journal. of Biomedical Research*, 2001, v. 58, I. 2, 180 – 187.
- [18] Temenoff JS, Lu L, Mikos AG. Bone tissue engineering using synthetic biodegradable polymer scaffolds. In: *Bone Engineering*, Davies JE (ed.), EM Squared, Toronto, 2000, pp. 455–462.
- [19] Cowin S.C., Van Burskirk W.C., Ashman R.B. *Properties of bone*. Ed. Shalak R, Chien S. *Handbook of Bioengineering*. USA, Mc Graw Hill, p. 21 (1987).